NANO LETTERS
Cite This: Nano Lett. 2019, 19, 116–123
Letter
pubs.acs.org/NanoLett

Synthesis of Patient-Specific Nanomaterials

James Lazarovits,[†] Yih Yang Chen,[†] Fayi Song,[†,‡] Wayne Ngo,[†] Anthony J. Tavares,[†] Yi-Nan Zhang,[†] Julie Audet,[†,§,∥] Bo Tang,[†,‡] Qiaochu Lin,[⊥] Mayra Cruz Tleugabulova,[⊥] Stefan Wilhelm,[†] Jonathan R. Krieger,[#] Thierry Mallevaey,[†,⊥] and Warren C. W. Chan*[,†,∥,○,¶]

[†]Institute of Biomaterials and Biomedical Engineering, University of Toronto, Rosebrugh Building, Room 407, 164 College Street, Toronto, Ontario M5S 3G9, Canada

[‡]College of Chemistry & Chemical Engineering, Chongqing University of Science & Technology, University Town, Shapingba District, Chongqing 401331, PR China

[§]Terrence Donnelly Center for Cellular and Biomolecular Research, University of Toronto, 160 College Street, Room 230, Toronto, ON M5S 3E1, Canada

[∥]Department of Chemical Engineering, University of Toronto, 200 College Street, Toronto, Ontario M5S 3E5, Canada

[⊥]Department of Immunology, University of Toronto, Medical Sciences Building, Room 7308, 1 King's College Circle, Toronto, ON M5S 1A8, Canada

[#]SPARC BioCentre, The Hospital for Sick Children, The Peter Gilgan Centre for Research & Learning, 686 Bay Street, 21st Floor Toronto, ON M5G 0A4 Canada

[○]Department of Chemistry, University of Toronto, 80 St. George Street, Toronto, Ontario M5S 3H6, Canada

[¶]Department of Materials Science and Engineering, University of Toronto, Wallberg Building, 184 College Street, Suite 140, Toronto, Ontario M5S 3E4, Canada

S *Supporting Information*

ABSTRACT: Nanoparticles are engineered from materials such as metals, polymers, and different carbon allotropes that do not exist within the body. Exposure to these exogenous compounds raises concerns surrounding toxicity, inflammation, and immune activation. These responses could potentially be mitigated by synthesizing nanoparticles directly from molecules derived from the host. However, efforts to assemble patient-derived macromolecules into structures with the same degree of size and shape tunability as their exogenous counterparts remains a significant challenge. Here we solve this problem by creating a new class of size- and shape-tunable personalized protein nanoparticles (PNP) made entirely from patient-derived proteins. PNPs are built into different sizes and shapes with the same degree of tunability as gold nanoparticles. They are biodegradable and do not activate innate or adaptive immunity following single and repeated administrations *in vivo*. PNPs can be further modified with specific protein cargos that remain catalytically active even after intracellular delivery *in vivo*. Finally, we demonstrate that PNPs created from different human patients have unique molecular fingerprints encoded directly into the structure of the nanoparticle. This new class of personalized nanomaterial has the potential to revolutionize how we treat patients and can become an integral component in the diagnostic and therapeutic toolbox.

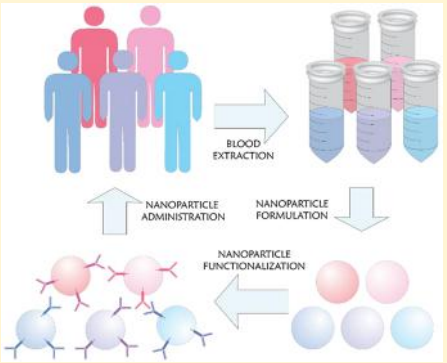

KEYWORDS: *Nanotechnology, personalized medicine, patient-specific nanomaterials, protein corona, protein nanoparticles, mass spectrometry*

Nanomaterials are integral components in the diagnostic and therapeutic toolbox and possess a unique set of optical, magnetic, and electrical properties that are derived from their material composition.[1] These parameters include the size, shape, and surface chemistry of the nanomaterial, all of which could dictate the biodistribution of the nanomaterial or its cellular interactions with the rest of the body.[2−4] Since these nanomaterials are similar in size to biological molecules, manipulating these physicochemical properties can theoretically control their transport to specific organs and cells. The core materials that have this high degree of synthetic tunability are built using substances that are exogenous to the body.[1] These include metals, polymers, and different carbon allotropes. When these foreign materials are assembled into nanoparticles greater than 6 nm, they cannot be renally excreted and are not eliminated from the body.[5] Therefore,

Received: August 23, 2018
Revised: November 30, 2018
Published: December 10, 2018

DOI: 10.1021/acs.nanolett.8b03434
Nano Lett. 2019, 19, 116–123

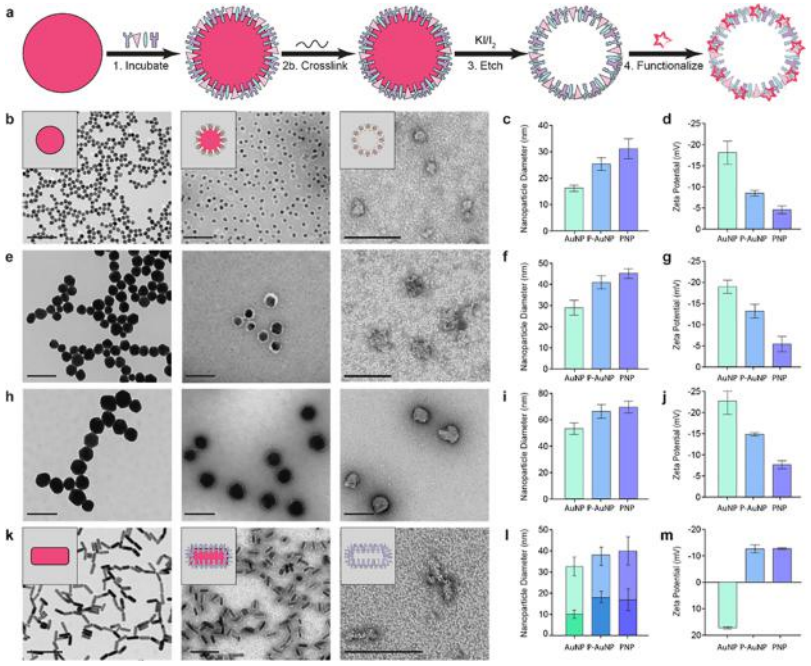

Figure 1. Engineering different sizes, shapes and compositions of personalized nanoparticles from human serum. (a) We expose gold nanoparticle (AuNP) templates to biological fluids, cross-link the surface-adsorbed proteins in place, and remove the metal core with etchants. Transmission electron microscopy images of (b) 15, (e) 30, and (h) 50 nm spheres and (k) 30 × 10 nm rod templates show one how to make PNPs in different sizes and shapes. (c, f, i, l) Spherical PNPs increased by 15 nm and rods by 7 nm at each axis. (d, g, j, m) Furthermore, spheres and rods assume surface charge densities between −8 and −15 mV following serum incubation and between −5 and −13 mV after etching, respectively. Error bars denote ± the standard deviation. Scale bar, 100 nm.

exposure to these nanomaterials raises numerous concerns surrounding toxicity, inflammation, and activation of innate or adaptive immunity, especially following repeated administrations.[6−11] In order to mitigate these side effects, several groups have used endogenous materials found within the body, such as lipids, to produce biocompatible nanoparticles.[12,13] Since the body contains a reservoir of many different types of endogenous building block materials, we can use this supply to build libraries of nontoxic and nonimmunogenic personalized nanostructures. However, current methods cannot produce personalized nanostructures with the same degree of size and shape tunability as their exogenous counterparts.[1] Here we demonstrate a solution to this problem with a simple three-step templating strategy to engineer personalized nanoparticles. These personalized nanoparticles have the same level of design freedom and complexity as exogenous nanomaterial classes while being nontoxic and nonimmunogenic.

Proteins are an abundant class of endogenous materials that can be exploited as building blocks for nanoparticle synthesis. Protein adsorption to nanoparticle surfaces is seen as a major problem for nanomaterial design,[14] because it obfuscates a nanoparticle's underlying synthetic properties. Previous work has shown that the types and abundances of proteins that adsorb to nanoparticles are predictable and reproducible, because it depends on the underlying nanoparticle size, shape, and surface chemistry.[14−19] However, we can neither prevent protein adsorption, nor has the field found a way to exploit it for a useful application. In this study, we discovered how to exploit protein adsorption on nanostructures to build personalized protein nanoparticles (PNP). To do this, we incubated nanoparticles with biological fluids that were isolated from animals and humans, cross-linked the surface-adsorbed proteins in place, and removed the internal nanoparticle core to leave a nanostructure composed entirely of endogenous and patient-derived proteins (Figure 1a). Since size, shape, and surface chemistry tunability depends on the nanoparticle core template, we used gold nanoparticles (AuNP) because they have the broadest size range of any nanomaterial (from 2 to 500 nm), can be constructed into many different shapes (rods, spheres etc.), and are readily surface-modified.[20−22] We combined the synthetic tunability offered by AuNPs with the phenomenon of protein adsorption to create PNP that have the same level of size and shape tunability as AuNP.

We began with AuNPs[20,21] that were 50 nm in diameter and coated them with pooled human serum. We separated the protein-coated AuNPs from unbound serum proteins using a rigorous centrifugation and washing protocol.[16] The surface-adsorbed proteins were cross-linked into a rigid "shell" using a photochemically activated, heterobifunctional, sulfo-LC-SDA cross-linker.[23] To make the PNP composed only of protein, we needed to remove the exogenous AuNP core. Cyanide-containing etching solutions have been used in templating strategies that incorporate nucleic acids[24] and polymers,[25] but they are hazardous to work with and irreversibly denature proteins.[26,27] Consequently, we chose an etching solution that contains potassium-iodide/iodine, because they do not form irreversible side chain adducts[27,28] (Figure 1b). After purification, we used inductively coupled plasma mass spectrometry to measure the atomic gold content of our PNP, and confirmed that PNP were essentially metal-free with roughly 35 ppb gold content (Figure S1). We also quantified the loss of gold and protein over the reaction and determined we achieved a 78% yield (Figure S2). Transmission electron microscopy revealed that PNP were size and shape tunable

DOI: 10.1021/acs.nanolett.8b03434
Nano Lett. 2019, 19, 116−123

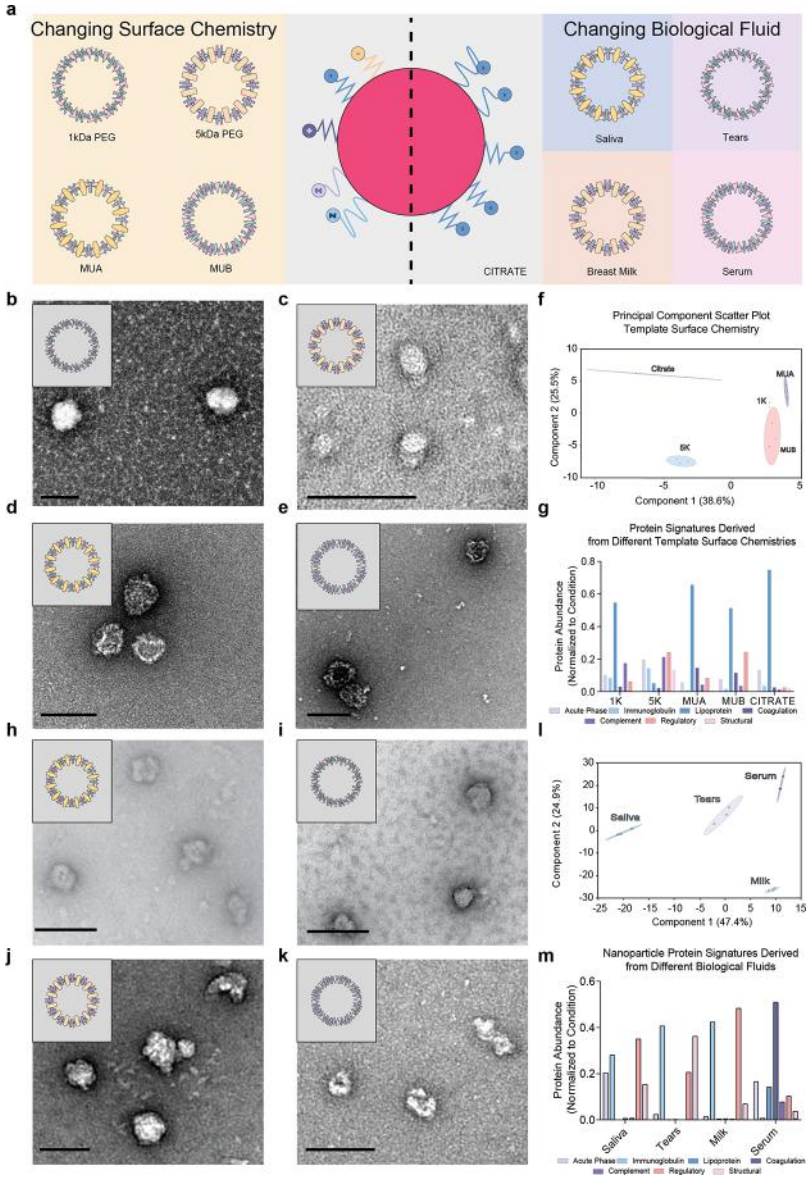

Figure 2. Engineering protein nanoparticles by changing template surface chemistry and source biological fluid. (a) Altering template surface chemistry to anionic, neutral, or cationic changes the distinct protein compositions found in PNPs. Different template surface chemistries such as (b) mercaptoundecanoic acid (MUA), (c) mercaptoundecyltrimethylammonium bromide (MUB), (d) 1 kDa polyethylene glycol (PEG), and (e) 5 kDa PEG produced reproducible PNP. (f) Principal component analysis (PCA) derived from mass spectrometry data with biological replicates (n = 3), shows the variability and statistically unique compositions derived from the different template surface chemistries. Colored circles represent the 95% confidence region for each replicate (n = 3). The greater the overlap between regions, the more similar they are. (g) The statistically significant proteins that were discovered using the multivariable analysis of variance were classified according to their gene ontology function using the Universal Protein Database. Similarly, (h) serum, (i) breast milk, (j) saliva and (k) tears were isolated from patients and used to make PNP. Each PNP was significantly different from one another according to (l) PCA and (m) multivariable analysis of variance. Scale bar, 100 nm.

because they remained spherical and consistently 15 nm larger than their AuNP templates. Their zeta potentials were always 7 mV less negative (Figure 1c,d, Figure S3, and Table S1). Overall, these results show a patient-derived nanostructure that is free of exogenous materials and approximates the template core size and morphology.

We next sought to expand our control over size and shape tunability. We therefore synthesized 15 and 30 nm spherical AuNPs, and 30 nm × 10 nm rod-shaped AuNPs.[29] We confirmed that PNPs were size and shape tunable, as spherical PNPs maintained the same 15 nm increase in diameter across all sizes (Figure 1, parts e, h, and k, and Table S1). On the basis of the unique geometry of the nanorod templates, we found they increased by 7 nm along both the longitudinal and transverse dimensions (Figure 1, parts f, i, and l, and Table S1). All PNP structures were 5.0 to 13.5 mV less anionic than their respective AuNP templates (Figure 1, parts g, j, m). Thus, we used AuNPs to build size and shape tunable PNPs.

Changing the composition of the adsorbed proteins influences biological fate.[14] It is also known that changing nanoparticle surface chemistry changes the enrichment pattern of proteins on the surface. Therefore, since different applications may require different compositions, we next explored the flexibility of our synthetic method by changing both the enrichment patterns of proteins, and the sources of the protein building blocks. We functionalized the surface of

DOI: 10.1021/acs.nanolett.8b03434
Nano Lett. 2019, 19, 116−123

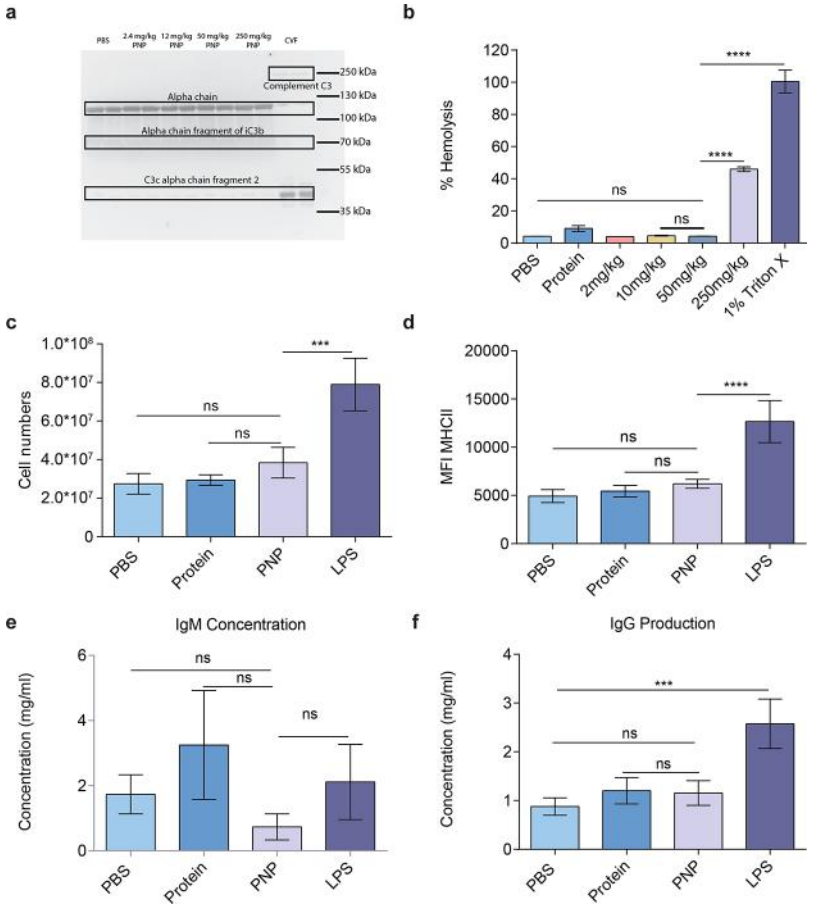

Figure 3. *In vitro* and *in vivo* toxicity and immunogenicity study of PNP. (a) PNPs did not visibly activate the complement system compared to PBS at four test concentrations of 5× (250 mg/kg), 1× (50 mg/kg), 0.2× (10 mg/kg), and 0.04× (2 mg/kg) compared to cobra venom factor (CVF). (b) At the same test concentrations, PNPs were found to be nonhemolytic compared to PBS or human serum until 5× the injected dose (****, $P < 0.0001$). (c) Splenocyte count shows two times more cells in the LPS group compared to the PNP group (***$P < 0.001$), and no statistical difference among PBS, PNP and free serum protein ($P > 0.05$). (d) LPS groups was higher than PNP groups, and no differences were found between PBS, PNP, and free serum for MHC II expression (****$P < 0.001$) and (e) total IgM and (f) IgG antibody production (***$P < 0.001$). All *in vitro* studies had three technical and two biological replicates. *In vivo* studies were $n = 4$ per condition. ± denotes standard deviation. Statistical significance was determined using one-way ANOVA with Tukey HSD correction for multiple comparisons.

50 nm AuNPs with neutral, anionic, or cationic ligands to modify the profile of adsorbed serum proteins species in order to yield compositionally distinct PNPs (Figure 2a).[14] We produced five unique classes of PNPs with different surface chemistries (Figure 2b–d) (see Materials and Methods and Table S2), and the proteins were analyzed using high resolution liquid chromatography tandem mass spectrometry. Each PNP had compositionally distinct protein populations (Figure S4). We confirmed each profile was distinct using both principal component (PCA) and canonical centroid analysis (CCA) (Figure 2, parts e and f, and Figure S5). Moving beyond serum, we next explored whether we could build PNPs from other biological fluids. We successfully engineered PNP from tears, saliva, and breast milk (Figure 2a). Each PNP contained a diverse array of protein building blocks that differed from one another in a statistically significant manner (Figure 2g–l and Figure S6). Interestingly, PNP size, shape, and charge remained constant regardless of the incubated biological fluid (Table S2). Since these PNPs consist of cross-linked self-proteins, we next tested the immunogenicity and toxicity of PNPs *in vitro* and *in vivo*.

Since PNPs built from serum contain complement proteins within their structure (Figure S4), we measured the dose-dependent relationship of serum-PNP on complement activation and hemolysis. We incubated 50 nm AuNP templates with isolated serum from inbred C57BL/6 mice to construct host-specific PNPs. We found that PNPs did not activate complement pathways nor induce hemolysis (Figure 3a). However, PNPs showed some hemolytic activity at a very high dose of 250 mg/kg (Figure 3b). We conjugated fluorescent dyes to the PNP (Figure S7) and used Förster resonance energy transfer (FRET)[30] (Figure S8) to show they degrade when exposed to Proteinase K (Figure S9). We then exposed bone-marrow derived dendritic cells to PNPs and found that they did not exhibit any measurable activation (Figure S10).[31,32]

After characterizing the safety and behavior of PNPs *in vitro*, we next performed both short-term and long-term studies in C57BL/6 mice *in vivo*. We first determined the short-term *in vivo* toxicity and immunogenicity by injecting C57BL/6 mice with 50 mg/kg of C57BL/6-PNPs. PNPs did not induce any liver toxicity (Figure S11) nor did they cause the production of chemokines and cytokines involved in early inflammation and immune responses (Figure S12). We next evaluated whether PNPs induced adaptive immunity following repeated administrations over a 28-day period. Mice were injected with 50

DOI: 10.1021/acs.nanolett.8b03434
Nano Lett. 2019, 19, 116–123

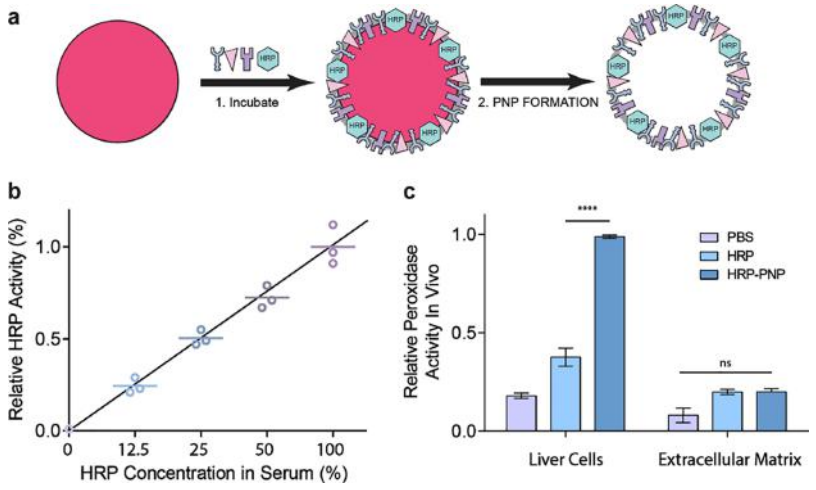

Figure 4. Functionalization and *in vivo* administration of different protein nanoparticle structures. (a) Horseradish peroxidase (HRP) can be mixed with serum in different amounts to create catalytically active PNPs. (b) The catalytic activity of the HRP-PNP can be linearly controlled by directly changing the concentration of HRP mixed with serum. (c) The robustness of the HRP integration into the PNP structures was confirmed following intravenous administration into C57BL/6 mice. HRP-PNP remained functional and preferentially distributed to liver cells rather than the extracellular matrix when compared to free HRP (n = 3). ± denotes standard deviation. Statistical significance was determined using an unpaired t test. ****P < 0.0001.

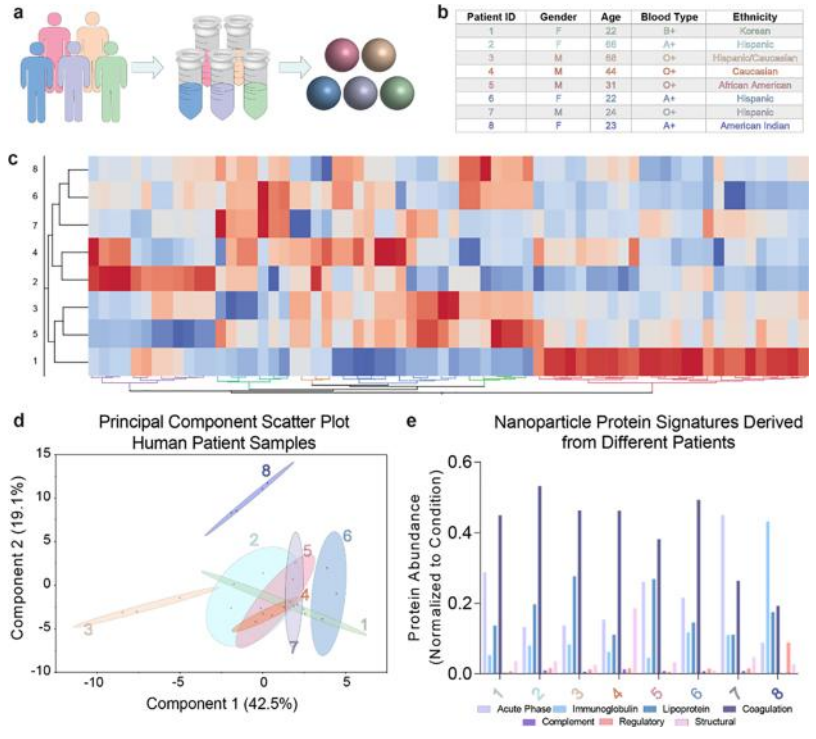

Figure 5. Different patient sera produces personalized nanoparticles with distinct molecular fingerprints encoded into the nanoparticle structure. (a) PNPs from eight different patients' sera (b) whose backgrounds extended over a diverse range of age, gender, and ethnicity. (c) Each patient has a distinct protein composition, which is presented in a hierarchically clustered heatmap. We include those proteins that are most significantly different among all patients (FDR P-value <0.05) (the color represents the Z-score where red is above the mean and blue is below the mean of the $\log_2$-based label free quantitative protein abundance intensity). (d) Personalization was confirmed using principal component analysis with biological replicates (n = 3). Colored circles represent the 95% confidence region for each patient replicate. The greater the overlap between regions, the more similar they are. (e) Statistically significant proteins were grouped based on eight specific biological functional categories (acute phase, immunoglobulin, lipoprotein, coagulation, complement, regulatory, and structural).

mg/kg of PNP, PBS, free serum protein, or a positive control of lipopolysaccharide (LPS) at 2 mg/kg on days 0 and 14. Their weights were recorded every 3 days. Mice treated with LPS lost 20% of their body weight 3 days after both the first and second injections (Figure S13), whereas PBS, protein, and PNP did not. Histopathology analysis indicated severe inflammation and neutrophil infiltration following LPS treatment, but no inflammation in the PBS, protein and PNP groups (Figure S14). Splenocytes were counted to determine the degree of immune cell recruitment, and we found no

DOI: 10.1021/acs.nanolett.8b03434
Nano Lett. 2019, 19, 116−123

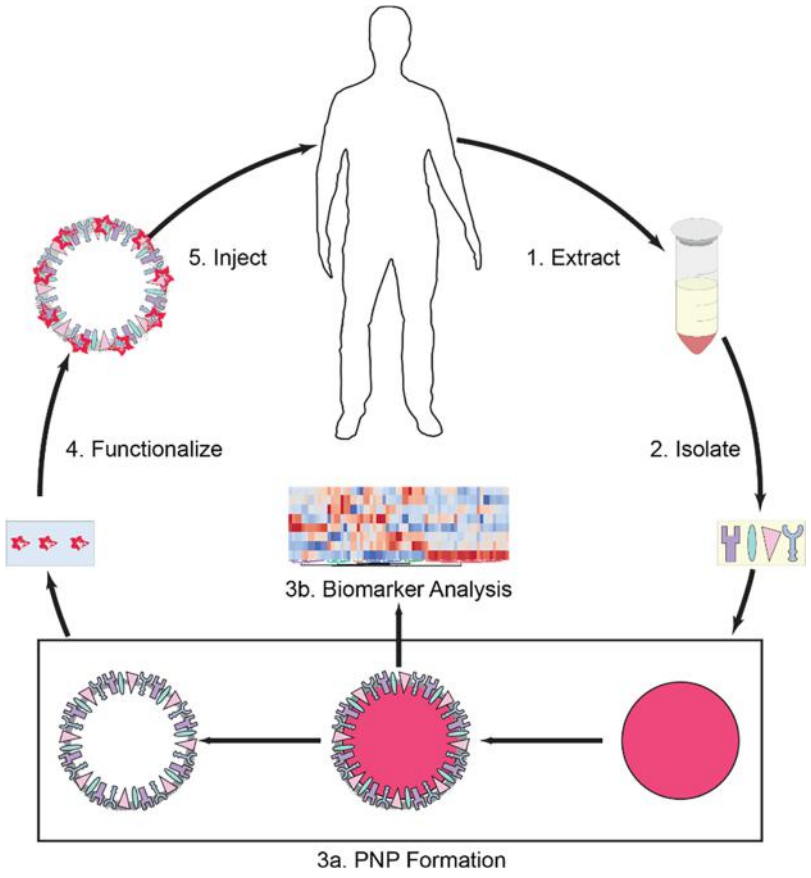

Figure 6. Schematic illustration of integrating patient-specific nanomaterials into a clinical setting. We envision that when patients are admitted into the hospital, and have their biological fluids retrieved, and then PNPs can be synthesized and functionalized according to the treatment or diagnostic need, and then readministered back into the patient in as little as 12 hours.

difference between PBS, protein, and PNP groups, but a 2-fold increased cell number was found in the LPS group (Figure 3C, $***P < 0.001$). Similarly, free proteins and PNPs did not upregulate expression of major histocompatibility class II (MHCII), CD86 or the activation marker CD69 by B ($B220^+$) cells (Figures 3d, S15, and S16).[33] This lack of B cell expansion and activation suggested that anti-PNP antibodies were unlikely to be produced. We similarly showed that neither free protein nor PNPs increased IgG or IgM production compared to the control (Figure 3e,f). Our results demonstrate that we can synthesize PNPs in microgram to milligram quantities, which do not activate innate or adaptive immune responses in mice, and may therefore be safe for long-term use *in vivo*.

In pursuit of future therapeutic and diagnostic applications, we next needed to engineer PNPs with greater complexity and functionality. We investigated whether we could exert direct control of the PNP composition, and incorporate biologically active macromolecules such as enzymes that can interact with the surrounding biological environment. We used horseradish peroxidase (HRP) as the model enzyme, since it generates a chromogenic signal that can be measured using spectrophotometry. In this synthetic process, HRP was initially mixed with serum, and this mixture was incubated with the AuNP template (Figure 4a). After synthesis and purification, we found that the enzymatic activity of the resulting HRP-PNP correlated linearly with the proportion of HRP initially spiked into the serum ($r^2 = 0.84$). (Figure 4b). We next exposed the HRP-PNP to serum and found it both remained catalytically active and resisted subsequent protein adsorption to the same degree as polyethylene glycol-conjugated AuNP (Figure S17). After confirming functional and structural stability, they were intravenously administered *in vivo*. HRP-PNP remained both catalytically active and were preferentially taken up by more cells compared to free HRP (Figure 4c, $P < 0.0001$). These results show these multicomponent PNP assemblies can be loaded with specific protein cargos that remain functionally intact even when delivered to cells inside of the body.

We exploited the predictable nature of protein−nanoparticle interactions to assemble patient-derived macromolecules into nanomaterials with the same design freedom and complexity as AuNP. Protein corona formation is well studied, but predominately seen as a bane to nanomaterial design. We have demonstrated how to convert this phenomenon into a solution to make a truly unique class of patient-specific nanoparticles. Specifically, PNP synthesis is highly robust as they can be engineered from different proteins and into varying sizes and shapes. Consequently, our strategy is generalizable and readily amenable to modifications. Future studies should explore ways to increase the complexity of the template, the types of integrated cargo, and how these features influence therapeutic efficacy, immunogenicity, and toxicity. Looking forward, we envision the PNP synthetic process will be integrated into the therapeutic and diagnostic workflow when patients visit the clinic or hospital. When patients visit, their biological fluids will be isolated and used to create a personalized treatment strategy (Figure S18). As a first step to explore this, we took sera from human patients from a

DOI: 10.1021/acs.nanolett.8b03434
Nano Lett. 2019, 19, 116−123

diverse range of ethnicity, age and gender, and synthesized their PNPs (Figure 5a,b). Each patient produced PNPs with distinct compositions (Figure 5c). Using PCA and CCA, we validated that this process was truly patient-specific. Each PNP contained a molecular fingerprint that could be used to discriminate each patient from the rest of the sample cohort (Figure 5d,e).

In the future, we envision that biological fluids will be isolated from patients, the PNPs designed with therapeutics and diagnostic agents, and then readministered into the patient for medical use (Figure 6). In addition, the protein biomarkers could be used to archive a patient's biological profile at the time of collection, monitor disease progression, or response to therapy.[34,35] This can be achieved because the personalized PNP contained a chemical signature that was unique to the patient. Interestingly, 100 of the proteins enriched from these biological fluids are known FDA clinical biomarkers (Table S3).[36] Overall, we have provided a generalized strategy to build patient-specific nanomaterials that can be used in therapeutic and diagnostic applications that will become integral components in the toolbox for personalized medicine.

■ ASSOCIATED CONTENT

Supporting Information

The Supporting Information is available free of charge on the ACS Publications website at DOI: 10.1021/acs.nanolett.8b03434.

Figures S1−19, Tables S1 and S2, and the materials and methods PDF)

Raw and processed proteomics analysis data (XLSX)

■ AUTHOR INFORMATION

Corresponding Author

*(W.C.W.C) E-mail: warren.chan@utoronto.ca.

ORCID

Warren C. W. Chan: 0000-0001-5435-4785

Author Contributions

J.L. and W.C.W.C. conceived the idea and wrote the manuscript. J.L., Y.Y.C., W.N., Y.-N.Z, J.A., M.C.T., J.R.K., T.M. and W.C.W.C. analyzed the data. J.L. conducted the experiments with support from Y.Y.C, W.N., Y.-N.Z, B.T., M.C.T., Q.L., F.S., A.J.T., S.W. and J.R.K. All authors read and commented on the manuscript.

Notes

The authors declare no competing financial interest.

Data Availability Statement: Authors can confirm that all relevant data are included in the paper and/or its Supporting Information files.

■ ACKNOWLEDGMENTS

The authors would like to thank C. Walkey, D. Holmyard, S. Chryssoulis, S. Sindhwani, S. Zhou, W. Poon, and B. Ouyang for their support and advice. The authors would also like to thank the Natural Sciences and Engineering Research Council (NSERC) and Canadian Institute of Health Research (CIHR) for funding support. J.L., Y.Y.C., W.N., Y.Z. thanks NSERC for graduate student fellowship. J.L. acknowledges Ontario Graduate Scholarship. A.J.T. acknowledges CIHR for post-doctoral fellowship.

■ REFERENCES

(1) Nel, A. E.; Mädler, L.; Velegol, D.; Xia, T.; Hoek, E. M. V.; Somasundaran, P.; Klaessig, F.; Castranova, V.; Thompson, M. *Nat. Mater.* **2009**, *8* (7), 543−557.

(2) Tenzer, S.; Docter, D.; Rosfa, S.; Wlodarski, A.; Rekik, A.; Knauer, S. K.; Bantz, C.; Nawroth, T.; Bier, C.; Sirirattanapan, J.; et al. *ACS Nano* **2011**, *5* (9), 7155−7167.

(3) Hong, M.; Zhu, S.; Jiang, Y.; Tang, G.; Pei, Y. *J. Controlled Release* **2009**, *133* (2), 96−102.

(4) Dai, Q.; Wilhelm, S.; Ding, D.; Syed, A. M.; Sindhwani, S.; Zhang, Y.; Chen, Y. Y.; Macmillan, P.; Chan, W. C. W. *ACS Nano* **2018**, *12*, 8423−8435.

(5) Soo Choi, H.; Liu, W.; Misra, P.; Tanaka, E.; Zimmer, J. P.; Itty Ipe, B.; Bawendi, M. G.; Frangioni, J. V. *Nat. Biotechnol.* **2007**, *25* (10), 1165−1170.

(6) Aillon, K. L.; Xie, Y.; El-Gendy, N.; Berkland, C. J.; Forrest, M. L. *Adv. Drug Delivery Rev.* **2009**, *61* (6), 457−466.

(7) Sayes, C. M.; Marchione, A. A.; Reed, K. L.; Warheit, D. B. *Nano Lett.* **2007**, *7* (8), 2399−2406.

(8) Alkilany, A. M.; Murphy, C. J. *J. Nanopart. Res.* **2010**, *12* (7), 2313−2333.

(9) Dobrovolskaia, M. A.; Germolec, D. R.; Weaver, J. L. *Nat. Nanotechnol.* **2009**, *4* (7), 411−414.

(10) Cho, W. S.; Cho, M.; Jeong, J.; Choi, M.; Cho, H. Y.; Han, B. S.; Kim, S. H.; Kim, H. O.; Lim, Y. T.; Chung, B. H.; et al. *Toxicol. Appl. Pharmacol.* **2009**, *236* (1), 16−24.

(11) Chen, Y. S.; Hung, Y. C.; Liau, I.; Huang, G. S. *Nanoscale Res. Lett.* **2009**, *4* (8), 858−864.

(12) Langer, K.; Balthasar, S.; Vogel, V.; Dinauer, N.; Von Briesen, H.; Schubert, D. *Int. J. Pharm.* **2003**, *257* (1−2), 169−180.

(13) Kooijmans, S. A. A.; Vader, P.; van Dommelen, S. M.; van Solinge, W. W.; Schiffelers, R. M. *Int. J. Nanomed.* **2012**, *7*, 1525−1541.

(14) Walkey, C. D.; Chan, W. C. W. *Chem. Soc. Rev.* **2012**, *41* (7), 2780−2799.

(15) Walkey, C. D.; Olsen, J. B.; Guo, H.; Emili, A.; Chan, W. C. W. *J. Am. Chem. Soc.* **2012**, *134* (4), 2139−2147.

(16) Walkey, C.; Olsen, J.; Song, F.; Liu, R.; Guo, H.; Olsen, W.; Cohen, Y.; Emili, A.; Chan, W. C. W. *ACS Nano* **2014**, *8* (3), 2439−2455.

(17) Lundqvist, M.; Stigler, J.; Elia, G.; Lynch, I.; Cedervall, T.; Dawson, K. A. *Proc. Natl. Acad. Sci. U. S. A.* **2008**, *105* (38), 14265−14270.

(18) Cedervall, T.; Lynch, I.; Lindman, S.; Berggård, T.; Thulin, E.; Nilsson, H.; Dawson, K. A.; Linse, S. *Proc. Natl. Acad. Sci. U. S. A.* **2007**, *104* (7), 2050−2055.

(19) Monopoli, M. P.; Walczyk, D.; Campbell, A.; Elia, G.; Lynch, I.; Baldelli Bombelli, F.; Dawson, K. A. *J. Am. Chem. Soc.* **2011**, *133* (8), 2525−2534.

(20) Frens, G. *Nature, Phys. Sci.* **1973**, *241*, 20−22.

(21) Perrault, S. D.; Chan, W. C. W. *J. Am. Chem. Soc.* **2009**, *131* (47), 17042−17043.

(22) Yeh, Y. C.; Creran, B.; Rotello, V. M. *Nanoscale* **2012**, *4* (6), 1871−1880.

(23) Gomes, A. F.; Gozzo, F. C. *J. Mass Spectrom.* **2010**, *45* (8), 892−899.

(24) Auyeung, E.; Cutler, J. I.; Macfarlane, R. J.; Jones, M. R.; Wu, J.; Liu, G.; Zhang, K.; Osberg, K. D.; Mirkin, C. A. *Nat. Nanotechnol.* **2012**, *7* (1), 24−28.

(25) Zhang, K.; Cutler, J. I.; Zhang, J.; Zheng, D.; Auyeung, E.; Mirkin, C. A. *J. Am. Chem. Soc.* **2010**, *132* (43), 15151−15153.

(26) Wood, M. A.; Riehle, M.; Wilkinson, C. D. W. *Nanotechnology* **2002**, *13* (5), 605−609.

(27) Fasco, M. J.; Stack, R. F.; Lu, S.; Hauer, C. R.; Schneider, E.; Dailey, M.; Aldous, K. M. *Chem. Res. Toxicol.* **2011**, *24* (4), 505−514.

(28) Ramachandran, L. *Chem. Rev.* **1956**, *56* (2), 199−218.

(29) Smith, D. K.; Korgel, B. A. *Langmuir* **2008**, *24*, 644−649.

DOI: 10.1021/acs.nanolett.8b03434
Nano Lett. 2019, 19, 116−123

(30) Yun, C. S.; Javier, A.; Jennings, T.; Fisher, M.; Hira, S.; Peterson, S.; Hopkins, B.; Reich, N. O.; Strouse, G. F. *J. Am. Chem. Soc.* **2005**, *127* (9), 3115−3119.
(31) Niikura, K.; Matsunaga, T.; Suzuki, T. *ACS Nano* **2013**, *7*, 3926−3938.
(32) Tarcha, P. J.; Chu, V. P.; Whittern, D. *Anal. Biochem.* **1987**, *165* (1), 230−233.
(33) Honda, S. I.; Sato, K.; Totsuka, N.; Fujiyama, S.; Fujimoto, M.; Miyake, K.; Nakahashi-Oda, C.; Tahara-Hanaoka, S.; Shibuya, K.; Shibuya, A. *Nat. Commun.* **2016**, *7*, 11498.
(34) Hajipour, M. J.; Laurent, S.; Aghaie, A.; Rezaee, F.; Mahmoudi, M. *Biomater. Sci.* **2014**, *2* (9), 1210−1221.
(35) Hadjidemetriou, M.; Al-ahmady, Z.; Buggio, M.; Swift, J.; Kostarelos, K. *Biomaterials* **2019**, *188*, 118−129.
(36) U.S. F.&D. Clinical Laboratory Improvement Amendments.

DOI: 10.1021/acs.nanolett.8b03434
Nano Lett. 2019, 19, 116−123